Separation Science and Technology
Publication details, including instructions for authors and subscription information:
http://www.informaworld.com/smpp/title~content=t713708471

THE EFFECT OF A SUPPORT LAYER ON THE PERMEABILITY OF WATER VAPOR IN ASYMMETRIC COMPOSITE MEMBRANES

Li Liu[a]; Yong Chen[a]; Shuguang Li[a]; Maicun Deng[a]
[a] Chinese Academy of Sciences, National Engineering Research Center of Membrane Technology, Dalian Institute of Chemical Physics, China

Online publication date: 31 December 2001

To cite this Article Liu, Li , Chen, Yong , Li, Shuguang and Deng, Maicun(2001) 'THE EFFECT OF A SUPPORT LAYER ON THE PERMEABILITY OF WATER VAPOR IN ASYMMETRIC COMPOSITE MEMBRANES', Separation Science and Technology, 36: 16, 3701 — 3720
To link to this Article: DOI: 10.1081/SS-100108357
URL: http://dx.doi.org/10.1081/SS-100108357

SEPARATION SCIENCE AND TECHNOLOGY, 36(16), 3701–3720 (2001)

THE EFFECT OF A SUPPORT LAYER ON THE PERMEABILITY OF WATER VAPOR IN ASYMMETRIC COMPOSITE MEMBRANES

Li Liu,* Yong Chen, Shuguang Li, and Maicun Deng

National Engineering Research Center of Membrane Technology, Dalian Institute of Chemical Physics, Chinese Academy of Sciences, China

ABSTRACT

Water vapor permeation through a silicone rubber–PSF (polysulfone) resistance composite membrane was studied. The resistance of the asymmetric composite membrane to the permeation of nitrogen, hydrogen, and water vapor is discussed on the basis of a serial resistance model. Compared with nitrogen and hydrogen, the resistance to water vapor is not attributable to the skin layer but is mainly due to the support layer of high water vapor permeability. The water vapor permeability decreases considerably with the increase of support layer resistance; the effect was greater when a relatively high vacuum was applied to the permeate gas side of the membrane. This result was also verified by the experiments of gas and vapor permeation through the composite membrane. In addition, the effects of the membrane structure on the water vapor permeability, as well as on the resistance of the support layer, were

*Corresponding author. E-mail: lli@dicp.ac.cn

also investigated. The membrane dehumidification process was used because it increased the porosity, the pore size of the support layer, and the thickness of the skin layer.

Key Words: Water vapor; Asymmetric composite membrane; Resistance; Support layer; Dehumidification process

INTRODUCTION

The membrane dehumidification process offers many advantages over the conventional processes, such as chemical absorption, physical adsorption, and cryogenic cooling (1–3). This dry method of purification is characterized as advantageous because no material is lost and no solvent is consumed through dehumidification. It can be operated continuously without the need for regeneration, has the potential to be highly energy efficient, is environmentally safe without generating secondary contaminants, and is efficient in terms of space and weight. Therefore, membrane dehumidification is a potential and rapidly developing process (4). Research on permeation behavior of water vapor was conducted to improve the comprehension of membrane dehumidification processes.

Presently, most of the gas separation membranes employed in industry, such as the Prism membrane, are composite membranes developed by Henis and Tripodi (5,6). Usually they have an asymmetric substrate with a thin dense surface layer on which the separation occurs and a porous layer that acts as a mechanical support. A high-flux and low-selectivity polymer is coated on the dense layer to plug a few defects. Generally, for the separation of permanent gases (e.g. O_2, N_2 and H_2), almost all the resistance of mass transfer is on the dense layer and the resistance of the support layer can often be neglected or its affect over-simplified in a permeation model. For this reason, most work is concentrated on the synthesis of polymers with high flux and selectivity (4) or on the preparation of membranes with defect-free thin dense layers (7).

However, recent studies have shown that the decrease in permeability for relatively fast gases, such as He and H_2, is attributed more or less to the support layer when the skin layer is very thin (8). Beuscher and Gooding have also found that the resistance of the support layer may reduce the sweep effect in the vapor permeation process (9,10).

Water vapor is more highly permeable through most of the polymer matrix, such as the polysulfone (PSF) and silicone rubber components, than the other permanent gases. In a composite membrane, the resistance distribution of water vapor may be different from that of the permanent gases, which have relatively low permeability. Although the dense layer is not thin, the resistance to water vapor

through the support layer may have great influence on the overall performance of the composite membrane.

In this paper, the effects of the support layer on water vapor permeability was investigated based on a serial resistance model, and the permeability of water vapor through the composite membrane under different pressures was measured to validate the resistance of the support layer.

THEORY

As shown in Fig. 1, the composite membrane has a PSF asymmetric substrate with a silicone rubber coating. The substrate is composed of a dense layer on the surface through which separation occurs, and a porous support layer that has a sponge structure to endure high pressure.

The resistance against gas flow can be expressed as a series circuit analogizing Ohm's law, and the total resistance is

$$R = R_1 + \frac{1}{\frac{1}{R_2} + \frac{1}{R_{31} + R_{32}}} + R_4 \tag{1}$$

The resistance of gases through the silicone rubber coating and the polymer phase of the PSF skin layer can be calculated by the following equations:

$$R_1 = \frac{L_1}{P_1(p) \cdot A} \tag{2}$$

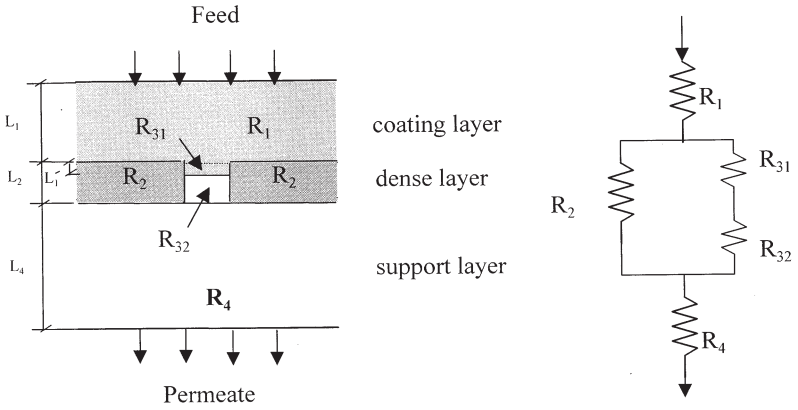

Figure 1. The resistance model for gas permeation through composite membranes.

MARCEL DEKKER, INC.
270 Madison Avenue, New York, New York 10016

$$R_2 = \frac{L_2}{P_2(p)\cdot A\cdot(1-\varepsilon')} \tag{3}$$

$$R_{31} = \frac{L_1'}{P_1(p)\cdot A\cdot\varepsilon'} \tag{4}$$

where L_1 and L_2 are the thickness of the coating layer and the dense layer respectively; L_1' is the length of silicone rubber coating plugging into the defective pores of the skin layer; A is the area of the membrane; and ε' is the porosity caused by the skin layer defects. When water vapor is permeating through membranes, clustering, condensation or swelling may occur due to molecular interactions (11–13). So the permeability coefficients $P_1(p)$ and $P_2(p)$ are not constants, just like those of N_2 and H_2, but depend on the feed pressure of water vapor. Based on an analogy of capillary flow, Carman suggested that gas permeation through any porous medium can be mainly controlled by viscous flow and Knudsen diffusion (14). The permeability of a gas through porous media can be estimated as

$$J_p = (am + bm^2)\cdot\frac{T}{T_0\times 76}\cdot\frac{\varepsilon}{L} \tag{5}$$

The first term accounts for viscous flow and the second term for Knudsen diffusion. The parameters a and b are given by

$$a = \frac{4}{3}\frac{\delta}{k_1}\frac{1}{q^2}\sqrt{\frac{8RT}{\pi M}} \tag{6}$$

$$b = \frac{1}{q^2}\cdot\frac{1}{k}\cdot\frac{1}{\mu}\cdot p_m \tag{7}$$

The relative parameters are average pore size m, porosity ε, tortuosity q, viscosity μ, mean pressure on the 2 side of the pores p_m, and shape factors k and δ/k_1. Carman suggested that for all porous membranes $\delta/k_1 = 0.8$ and $k = 2.5$.

Therefore the resistance of gases through the defective pores of the PSF skin layer and the support layer can be expressed as

$$R_{32} = \frac{L_2 - L_1'}{(am' + bm'^2)\cdot A\cdot\dfrac{T}{T_0\times 76\cdot\varepsilon'}} \tag{8}$$

$$R_4 = \frac{L_4}{(am + bm^2)\cdot A\cdot\dfrac{T}{T_0\times 76}\cdot\varepsilon} \tag{9}$$

The gas permeability rate J is the ratio of the permeation flux Q and the pressure difference Δp. It varies inversely with total resistance

$$J = \frac{Q}{A\cdot\Delta p} = \frac{1}{R\cdot A} \tag{10}$$

MARCEL DEKKER, INC.
270 Madison Avenue, New York, New York 10016

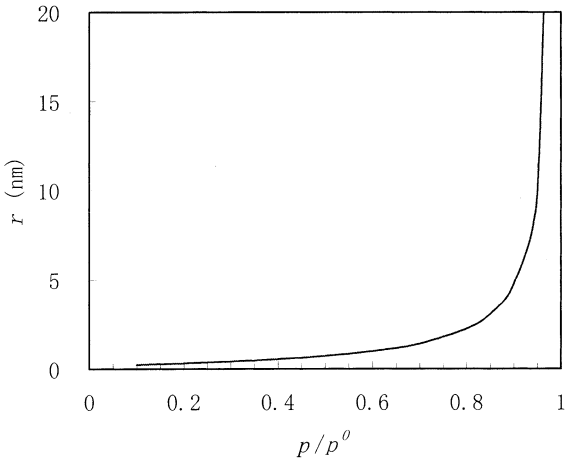

Figure 2. The maximum pore size in which condensation may occur under different feed pressures.

The relationship between water vapor pressure and the maximum pore in which capillary condensation may occur can be described by the Kelvin equation

$$\ln \frac{p}{p^0} = -\frac{2\sigma \cdot \cos\theta}{r} \cdot \frac{V_m}{RT} \tag{11}$$

p^0 is the saturated pressure of water vapor under operation temperatures; σ is surface tension; r is the maximum pore in which condensation may occur; and V_m is the mol volume of water. By means of Eq. (11), the maximum pore size in which condensation may occur under different feed pressures was calculated and is shown in Fig. 2.

From Fig. 2. one can see that when relative pressure $p_1/p^0 < 0.9$ capillary condensation could not occur unless the pore size is less than 5 nm, which is much less than the average pore size in the support layer. So in this work, although capillary condensation does occur in some small pores of the membrane, its effects on the permeability could be neglected because the size of the support layer is relatively very large.

EXPERIMENTAL

Membrane Preparation

Dense PSF and silicone rubber films were made by the solution casting method. The polymer solution was cast on glass plates, and the solvents were

evaporated for more than 4 hours when the glass was heated to 95°C. Then the films were set in a vacuum oven to dry for more than 4 days at 140°C.

The hollow fiber composite membrane is prepared by spinning the PSF asymmetric hollow fiber membrane from a "dry-wet" type dope and coating it with a silicone rubber solution. The fiber dimension was approximately 450 μm o.d. and approximately 150–220 μm i.d. A membrane module was made for the permeability measurement.

Permeability Measurement

The gas permeability through the dense polymer films was measured at 30°C on the G.T.R. Measurement Apparatus (RSK Model K-315N-01, Rikaseiki Kogyo Co, Ltd) shown in Fig. 3. Upstream of the permeation cell was a liquid water vial, a ballast volume, and a vacuum gauge with a range of approximately 0–10 kPa. Downstream of the permeation cell was a receiving tank and a pressure transducer that was operated over the range of approximately 0–1.33 kPa. The temperature of permeation cell was controlled at 30 ± 0.5°C. First, the system was evacuated to the pressure less than 1.5 Pa by a vacuum pump. Then water vapor was sent into the feed side of film. With the permeation of water vapor, the pressure of the permeate side increased gradually. The permeation coefficients were calculated by measuring the increasing pressure on the permeate side over time.

The equipment for the permeability measurements of hollow fiber is shown in Fig. 4. Permeating water vapor was condensed with a liquid nitrogen trap. The permeability of water vapor was calculated by the weight of collected water. The

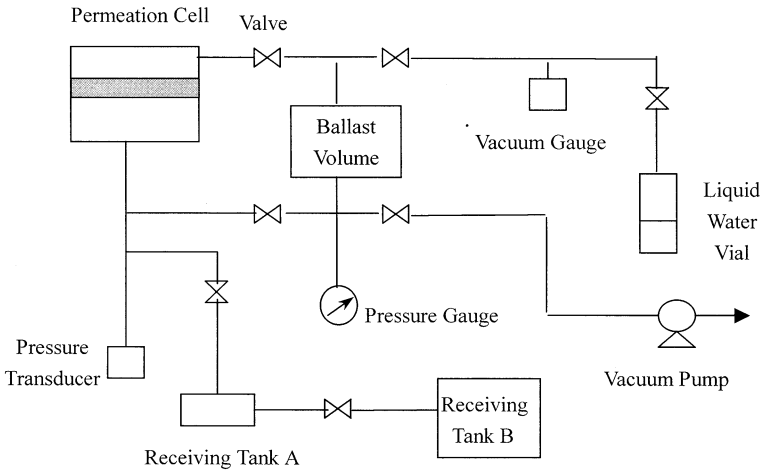

Figure 3. Schematic of film permeation apparatus.

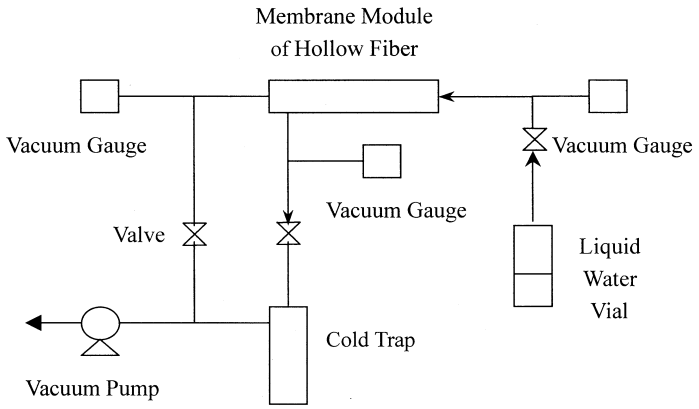

Figure 4. Schematic of membrane permeation apparatus for hollow fiber modules.

pressures of both sides of the membrane were controlled by needle valves, and they were measured by a vacuum gauge within a range of approximately 0–10 kPa. The temperature of the membrane module was also controlled at 30 ± 0.5°C. Experimental errors were no more than 10%.

RESULTS

Permeation Coefficient of Polymer Film

As shown in Fig. 5, the permeation coefficient of water vapor, $P_2(p)$, through dense PSF is approximately 3.5–4.0 × 10^{-7} $cm^3 \cdot cm/cm^2 \cdot s \cdot kPa$ at

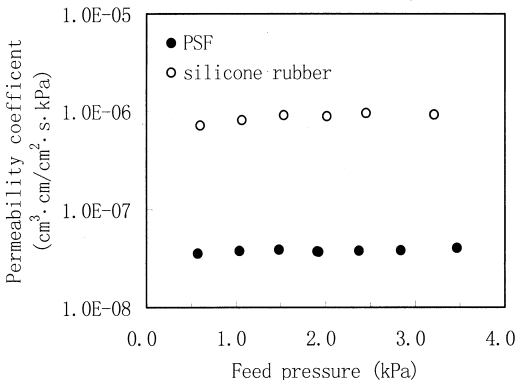

Figure 5. The permeability coefficient of water vapor through dense PSF and silicone rubber films.

MARCEL DEKKER, INC.
270 Madison Avenue, New York, New York 10016

Table 1. The Performance of PSF-Silicone Rubber Hollow Fiber Composite Membranes

Membrane	Condition	J_{H_2} $cm^3/cm^2 \cdot s \cdot kPa$	J_{N_2} $cm^3/cm^2 \cdot s \cdot kPa$	Selectivity
No. 1	Uncoated	1.52×10^{-3}	3.62×10^{-4}	4.2
	Coated	6.20×10^{-5}	1.00×10^{-7}	61.5
No. 2	Uncoated	1.43×10^{-4}	3.57×10^{-5}	4.0
	Coated	2.33×10^{-5}	3.98×10^{-7}	58.6
No. 3	Uncoated	1.16×10^{-3}	3.89×10^{-4}	3.0
	Coated	4.19×10^{-5}	9.17×10^{-7}	45.7

Uncoated denotes PSF asymmetric membranes without silicone rubber coating.
Coated denotes PSF asymmetric membrane coated by silicone rubber.

30°C, which is not a strong function of feed pressure on a large-activity scale. The permeation coefficient of water vapor through silicone rubber, $P_1(p)$, is approximately 7.1–9.2 $\times 10^{-6}$ $cm^3 \cdot cm/cm^2 \cdot s \cdot kPa$, which slightly increases with the increase of feed pressure. This result is consistent with that of Baker et al. by the Toepler pump method (15).

The Performance of Hollow Fiber Composite Membrane

Table 1 shows the performance of hollow fiber composite membranes of silicone rubber- PSF that were used in the experiment.

Estimate of Membrane Structure Parameters

A H_2-N_2 selectivity value of 61.5 of membrane No. 1 of Table 1 suggests that the composite membrane is essentially defect free. The structure parameters of the dense layer and the coating layer can be estimated by the method outlined in (16) by means of H_2 and N_2 performance. A detailed description of the method can be seen in appendix A. The results show the following approximate parameters: coating thickness = 0.5 μm; PSF dense layer = 0.05 μm; average pore size of defect on the dense layer = 0.02 μm; and porosity = 1.0×10^{-6}. We assumed that support layer resistance to H_2 was less than 5% and that its resistance to N_2 can be neglected under relatively high pressure. Based on the resistance model and the permeability values of H_2 and N_2 as calculated from Eqs. (1,9, and 10), we determined an average pore size of 0.09 μm and a porosity of 1.7×10^{-2} for the porous support layer. The total thickness of the membrane, measured by microscope was approximately 115, which approximately equals the thickness of the support layer because of the thin dense and coating layers.

Marcel Dekker, Inc.
270 Madison Avenue, New York, New York 10016

The Resistance of Support Layer to Gases

The support layer resistance to gases was calculated through the use of membrane structure parameters, which were obtained from the evaluation and measurements described for membrane No. 1. The mean pressure on both sides of the support layer p_m is defined as the arithmetic average of the pressure in the permeation side and the pressure of the interface between the dense layer and the support layer. Detailed calculations of p_m are shown in appendix B. The ratio of gas resistance between the support layer and the total resistance R_4/R, as well as the permeability J through composite membrane, under different p_m values can be seen in Figs. 6 and 7.

Based on the structure parameters calculated for membrane No. 1, the permeability of water vapor, N_2, and H_2 passing through the skin or support layer were calculated by Eqs. (1,2,3,9, and 10) (Table 2). No remarkable difference among the permeability values of water vapor, H_2, and N_2 passing through the support layer with porous flow were found, but the sequence of permeability through the dense layer was $J_{\text{water vapor}} >> J_{H_2} >> J_{N_2}$. The resistance of the support layer to water vapor R_4 was approximately 40%–95% of the total resistance R, which was the highest among the 3 gases studied.

Gas flow can be mainly explained by viscous flow and Knudsen diffusion in the support layer. The permeability of the viscous-flow mode is higher than that of the latter. At relatively low pressures, low permeability is mostly attributed to Knudsen flow because of the high mean free path. As the pressure in the system increases (i.e., mean free path decreases), the Knudsen flow eventually transits into a viscous flow where the permeability increases and the resis-

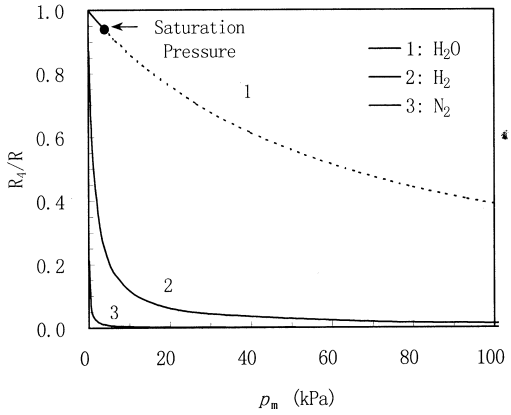

Figure 6. The ratio of gas resistance on the support layer to the total resistance, R_4/R, as a function of average pressure p_m.

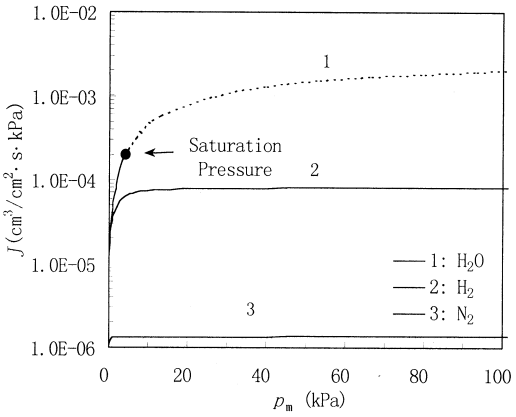

Figure 7. The permeability rate of nitrogen, hydrogen, and water vapor as a function of average pressure p_m.

tance decreases. The permeability values of H_2 and N_2 are independent of the operation pressure because the PSF dense layer determines their performances at not very low pressures. However, the high water-vapor permeation coefficient in PSF contributes to the important role of the support layer in the total resistance of the membrane.

Because the average pressure on both sides of the support layer is no higher than 4.24 kPa, the saturation pressure of water vapor at 30°C, the support layer resistance is greater than 90% for the permeation of pure water vapor (Fig. 6). Moreover, Fig. 8 clearly demonstrates that the permeability of water decreases 10–90 times because of the resistance of the support layer.

For dehumidification processes based on membranes, a vacuum system is often used to improve the differential pressure (i.e., to increase the driving force). This will reduce the permeability of water vapor according to the analysis above.

Table 2. The permeability of Water Vapor, N_2, and H_2 Passing Through Skin or Support Layer

	Permeability ($cm^3/cm^2 \cdot s \cdot cmHg$)		
Gases	Skin layer	Support layer	Composite membrane
H_2O	4.44×10^{-3}	1.89×10^{-4}	1.81×10^{-4}
N_2	1.79×10^{-6}	1.07×10^{-4}	1.75×10^{-6}
H_2	1.11×10^{-4}	2.27×10^{-4}	6.76×10^{-5}

$P_m = 2.7$ kPa.

MARCEL DEKKER, INC.
270 Madison Avenue, New York, New York 10016

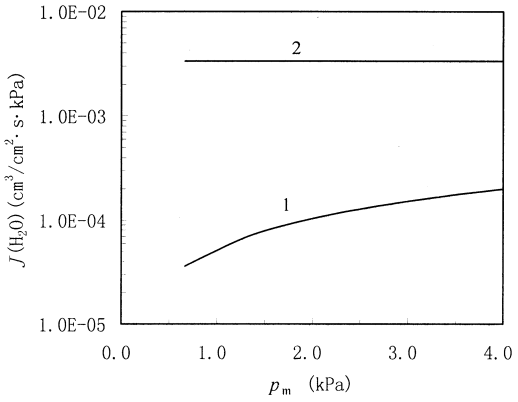

Figure 8. The influence of the support layer on water vapor permeation through the composite membrane: 1) with the resistance of support and 2) without the resistance of support layer.

Experimental Verification

The permeability values of water vapor, determined by both experimental data and calculations based on the resistance model, through silicone rubber–PSF hollow-fiber composite membrane under different mean pressures on both sides of the support layer p_m are shown in Fig. 9. The figure shows that the calculated

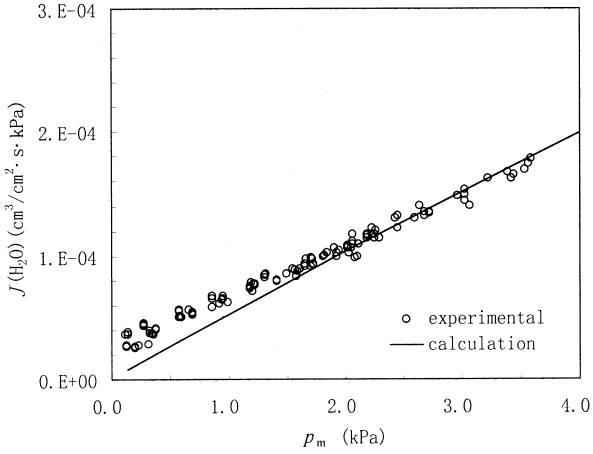

Figure 9. Water vapor permeability in hollow-fiber composite membrane by the experimental data and calculations under different mean pressures on both sides of the support layer p_m.

MARCEL DEKKER, INC.
270 Madison Avenue, New York, New York 10016

Table 3. The Thickness Estimates of the PSF Dense Layer and Silicone-Rubber Coating Layer

Membrane	Thickness of Silicone Rubber Coating Layer (μm)	Thickness of PSF Dense Layer (μm)	Thickness of Silicone Rubber-PSF
No. 2	~2	~0.2	>10
No. 3	~2	~0.1	>20

and experimental data are almost consistent with each other. So we induced that the support layer resistance mainly controls water vapor permeation. The slight difference between data sets is probably the result of 2 assumptions made in the experimental design: First, mean pore size was adopted in the model and so the wide distribution of pore sizes was not regarded. Second, only Knudsen and viscous flows were considered; surface diffusion, capillary condensation, and other mechanisms that might have also had some impact on water vapor permeation.

Table 3 shows the thickness of the PSF dense layer and the silicone rubber coating layer, estimated by the performances of N_2 and H_2 as listed in Table 1 for membrane No. 2 and No. 3. If the water vapor resistance was mainly on the skin layer, like in the case of N_2 and H_2, the permeability of water vapor (Table 4) could be evaluated based on the water vapor permeation coefficients of polymer films and the membrane structure parameters noted in Table 3. From Table 4, one can see that the expected permeability values of water vapor through the uncoated membrane are approximately 1.9×10^{-2} cm^3 /cm^2·s·kPa and 4.1×10^{-2} cm^3 /cm^2·s·kPa under $p_m = 2.7$ kPa on membranes No. 2 and No. 3, respectively, and on both membranes the permeability values decrease approximately 30%–50% after they are coated. On the contrary, the experimental permeability values of

Table 4. The Expected Permeability Values of Water Vapor Through Uncoated and Coated Membranes Assuming That the Resistance Is Mainly on the Skin Layer

	Expected Permeability (cm^3 /cm^2·s·kPa)	
Membranes	Uncoated	Coated
No. 2	1.9×10^{-2}	1.3×10^{-2}
No. 3	4.1×10^{-2}	2.0×10^{-2}

*$p_m = 2.7$ kPa.

MARCEL DEKKER, INC.
270 Madison Avenue, New York, New York 10016

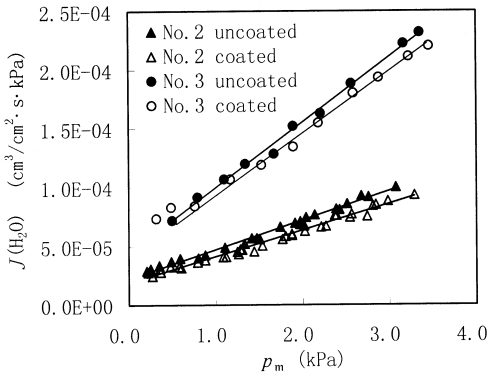

Figure 10. Comparison of water vapor permeability through coated and uncoated membranes.

coated or uncoated hollow-fiber membrane at a side range of pressures (Fig. 10), are nearly 2 orders of magnitude lower than the expected results. Most important, the permeability of experimental membranes decreased relatively little after being coated. The great inconsistency between expected and experimental results showed that the incorrectness of the assumption that the resistance is mainly on skin layer. Therefore, the resistance of water vapor through the dense layer and the coating layer can be neglected, and it is the support layer, in fact, that controls water vapor permeation.

THE EFFECTS OF MEMBRANE STRUCTURE PARAMETERS

Porosity of the Support Layer

The estimated structure parameters of membrane No. 1 were studied. Although support layer resistance is reduced and water vapor permeability is increased with porosity increases of the support layer, as shown in Figs. 11 and 12, the resistance of the support layer is not less than 90% of the total resistance until the porosity reaches 10^{-2}. If the porosity increases to values greater than 10^{-2}, the resistance reduces rapidly.

The increase in porosity will lead to high water-vapor permeability, but for gases like nitrogen and methane that possess relatively low permeability, only small changes will be exhibited. So the enhancement in porosity will lead to a great improvement of the selectivity between water vapor and nitrogen or methane in dehumidification processes.

MARCEL DEKKER, INC.
270 Madison Avenue, New York, New York 10016

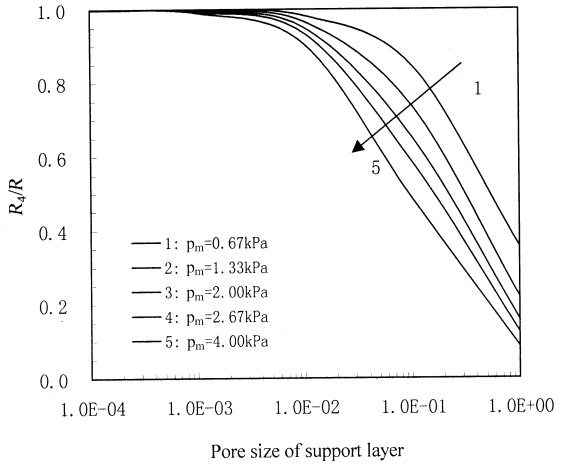

Figure 11. The support layer resistance to water vapor permeation as a function of support layer porosity.

Average Pore Size of the Support Layer

All the parameters studied, except average pore size, were based on the structure parameters of membrane No. 1. The support layer resistance reduces and the water vapor permeability increases with the increase of pore size in the sup-

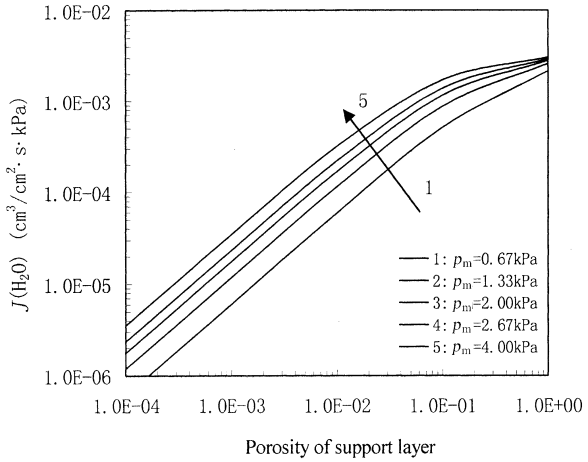

Figure 12. The permeability rate of water vapor as a function of support layer porosity.

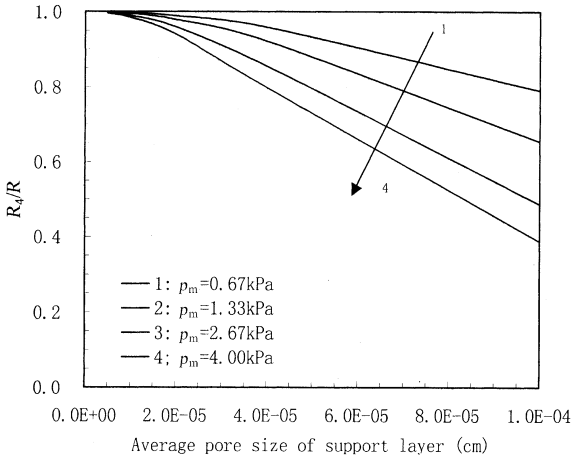

Figure 13. The water vapor resistance through the support layer as a function of the average pore size of the support layer.

port layer, as shown in Figs. 13 and 14. The permeability improves greatly at increased pore sizes until the pore size is larger than approximately 0.2–0.4 μm. For this reason, the selectivity of water vapor with nitrogen could also be increased by enhancing the pore size.

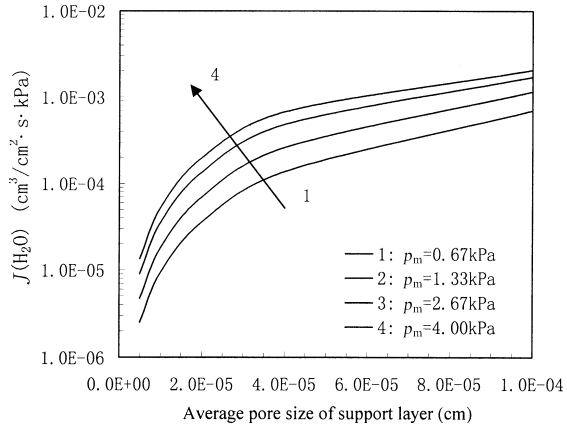

Figure 14. The water vapor permeability as a function of the average pore size of the support layer.

MARCEL DEKKER, INC.
270 Madison Avenue, New York, New York 10016

Therefore, increasing the porosity and pore size of the support layer is believed to increase the permeability of water vapor. However too high a porosity, especially that caused by high pore sizes of the support layer will decrease the strength of membranes.

Thickness of the Dense Layer

Usually, reducing the skin layer thickness is an effective way for separating N_2, H_2, and O_2 because the resistance of the membrane is focused mainly on the skin layer. However, the resistance is not the primary source of resistance for water vapor.

The permeability of water vapor and nitrogen through the skin layer is illustrated in Fig. 15. The thickness has little influence on the water vapor permeability, while the nitrogen permeability decreases greatly with increased skin layer thickness.

Therefore, we have drawn a different conclusion from that of the traditional gas separation processes for the separation of water vapor and nitrogen, i.e., the selectivity is high under a large thickness of the skin layer for water and nitrogen. Therefore, at the specified conditions, the increase in the thickness of the skin layer is advantageous for the dehumidification process based on membrane separation. Maintaining membrane strength would be easier when thick skin layers are used for effective separation than when increased porosity and pore size of the support layer are used to increase permeability.

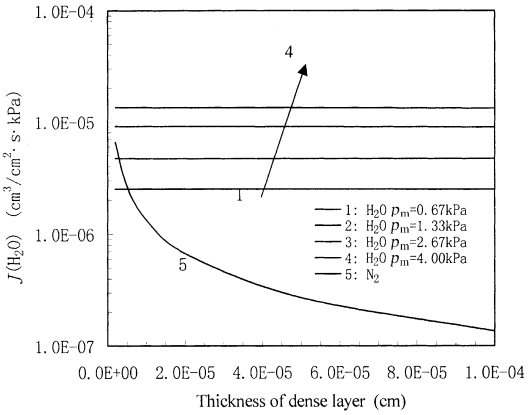

Figure 15. The permeability of water vapor and nitrogen as a function of the dense layer thickness.

MARCEL DEKKER, INC.
270 Madison Avenue, New York, New York 10016

CONCLUSIONS

The permeation behavior of water vapor through asymmetric composite membranes is different from that of the permanent gases, as the permeability of the latter is nearly independent of the membrane support layer. In the silicone rubber–PSF system, experiment results showed that support layer resistance caused the water vapor permeability to decrease greatly. Results from both simulated models and experiments supported this conclusion.

The nearly equal permeability of water vapor through hollow fiber membranes coated with silicone rubber or without coating also verified that the support layer mainly controls water vapor permeation.

The membrane configuration has a great impact on water vapor permeability. The increased porosity and pore size of the support layer favor resistance reduction of the support layer and improved water vapor permeability. An increase in the thickness of the skin layer reduces nitrogen permeability but has almost no influence on water vapor permeability. This information will allow for enhanced dehumidification processes through optimized membrane-structure parameters.

APPENDIX A: EVALUATING MEMBRANE STRUCTURE PARAMETERS

N_2 and H_2 resistance through support layer is neglected when evaluating the structure parameters of skin layer and coating layer. So, in Eq. (1)

$$R_4 = 0 \tag{12}$$

From equation (10)

$$R = \frac{1}{J \cdot A} \tag{13}$$

The skin layer porosity is very low, less than 10^{-6}, and $L_1 >> L_2$. Therefore, the change of L_1' has little influence on gas permeability through the composite membrane (17); $L_1' = L_1$.

Through the combination of Eqs. (1–4), the permeability of gases through composite membrane can be expressed as

$$\frac{1}{J^c} = \frac{L_1}{P_1(p)} + \frac{L_2}{P_2(p) \cdot (1 - \varepsilon') + P_1(p) \cdot \varepsilon'} \tag{14}$$

By combining Eqs. (1,3, and 8), one can express the permeability of gases through uncoated membranes as

$$\frac{1}{J} = \frac{L_2}{P_2(p) \cdot (1 - \varepsilon') + (am' + bm'^2) \cdot \dfrac{T}{T_0 \times 76} \cdot \varepsilon'} \tag{15}$$

MARCEL DEKKER, INC.
270 Madison Avenue, New York, New York 10016

For 1 hollow-fiber membrane module, the permeability values of H_2 and N_2 with coating are $J^c_{H_2}$, $H^c_{N_2}$ and without coating are J_{H_2}, H_{N_2}. With these 4 permeability values plugged into Eqs. (14 and 15), m', ε', L_1, and L_2 can be resolved.

APPENDIX B: THE CALCULATION OF AVERAGE PRESSURE OF SUPPORT LAYER p_m

In the composite membrane shown in Fig. 1, the pressure distribution p_1, p_1 and $p_3 \cdot p_1$, and p_3 are defined as the feed-side and permeate-side pressures of composite membrane, respectively, while p_2 is the pressure of the interface between dense layer and support layer. Q_1 and J_1 are the flow flux of gases passing through the skin and coating layers. Q_2 and J_2 are the flow flux and permeability of gases passing through the support layer. Because

$$Q_1 = J_1 \cdot A \cdot (p_2 - p_1) \tag{16}$$

$$Q_2 = J_2 \cdot A \cdot (p_3 - p_2) \tag{17}$$

$$Q_1 = Q_2 \tag{18}$$

$$\frac{1}{J_1 A} = R_1 + \frac{1}{R_2 + \dfrac{1}{R_{31} + R_{32}}} \tag{19}$$

$$\frac{1}{J_2 A} = R_4 \tag{20}$$

$$p_m = \frac{(p_2 + p_3)}{2} \tag{21}$$

p_1 and p_2 can be measured experimentally and Eqs. (1–9) and (16–21) can be solved for p_2 and p_m.

NOMENCLATURE

A	membrane area (cm^2)
J	permeability rate ($cm^3/cm^2 \cdot s \cdot cmHg$)
K_1	shape factor
L_1	the thickness of coating layer (cm)
L_1'	the length of silicone coating used to plug the defect pores of the dense layer (cm)
L_2	the thickness of dense layer (cm)
M	molecular weight
m	average pore size of support layer (cm)
m'	average pore size of skin layer (cm)

MARCEL DEKKER, INC.
270 Madison Avenue, New York, New York 10016

p	operation pressure (kPa)
p^0	saturated pressure (kPa)
p_m	the mean pressure on the two sides of pore (kPa)
P_1, P_2	permeation coefficients of silicone rubber and PSF ($cm^3 \cdot cm/cm^2 \cdot s \cdot kPa$)
q	tortuosity
Q	gas permeation flux (cm^3/s)
r	pore size of capillary (m)
R	resistance of gas permeation ($s \cdot kPa/cm^3$)
T	temperature (K)
T_0	standard temperature (273K)
V_m	mol volume (cm^3/mol)
δ/k_1	shape factor
θ	contact angle
σ	surface tension (N/m)
ε	porosity of support layer
ε'	porosity of skin layer
μ	viscosity (Pa·s)

ACKNOWLEDGMENTS

The authors thank the Membrane Center of the Dalian Institute of Chemical Physics for providing the hollow fiber membranes.

REFERENCES

1. Rice, A.W.; Murphy, M.K. Gas Dehydration Membrane Apparatus. US Patent 4,783,201, November 8, 1988.
2. Overmann, D.C. Membrane Process for Removing Water Vapor from Gas. US Patent 5,034,025, July 23, 1991.
3. Bikson, B.; Giglia, S.; Nelson, J.K. Process for Dehydration of Gas and Composite Permeable Membranes. US Patent 5,067,971, November 26, 1991.
4. Stern, S.A. Polymer for Gas Separations: The Next Decade. J. Memb. Sci. **1994,** *94*, 1–65.
5. Henis, J.M.S.; Tripodi, M.K. Composite Hollow Fiber Membranes for Gas Separation: The Resistance Model Approach. J. Memb. Sci. **1981,** *8,* 233–246.
6. Henis, J.M.S.; Tripodi, M.K. A Novel Approach to Gas Separation Using Composite Hollow Fiber Membranes. Sep. Sci. Technol. **1980,** *15*, 1059–1068.

MARCEL DEKKER, INC.
270 Madison Avenue, New York, New York 10016

7. Pesek, S.C.; Koros, W.J. Aqueous Quenched Asymmetric Polysulfone Hollow Fibers Prepared by Dry/Wet Phase Separation. J. Memb. Sci. **1994,** *88,* 1–19.
8. Clausi, D.T.; McKelvey, S.A.; Koros, W.J. Characterization of Substructure Resistance in Asymmetric Gas Separation Membranes. J. Memb. Sci. **1999,** *160*, 51–64.
9. Beuscher, U.; Gooding, C.H. Characterization of the Porous Support Layer of Composite Gas Permeation Membranes. J. Memb. Sci. **1997,** *132*, 213–227.
10. Beuscher, U.; Gooding, C.H. The Influence of the Porous Support Layer of Composite Membranes on the Separation of Binary Gas Mixtures. J. Memb. Sci. **1999,** *152*, 99–116.
11. Schult, K.A.; Paul, D.R. Water Sorption and Transport in a Series of Polysulfones. J. Polym. Sci. Part B: Polym. Phy. **1996,** *34*, 2805–2817.
12. Cha, J.S.; Li R.; Sirkar, K.K. Removal of Water Vapor and VOCs from Nitrogen in Hydrophilic Hollow Fiber Gel Membrane Permeator. J. Memb. Sci. **1996,** *119*, 139–153.
13. Yang, D.K.; Koros, W.J.; Hopfenberg, H.B.; Stannett, V.T. Sorption and Transport Studies of Water in Kapton Polymide I. J. Appl. Polym. Sci. **1985,** *30*, 1035–1047.
14. Carman, P.C. *Flow of Gases through Porous Media*; Butterworth Publications: London, 1956.
15. Baker, R.W.; Yoshioka, N.; Mohr, J.M.; Khan, A.J. Separation of Organic Vapors from Air. J. Memb. Sci. **1987,** *31*, 259–271.
16. Lu, W.J.; Liu, L.; Wang, H.; Ma, M.J. The Structure Parameters Determination of Asymmetric Membranes and Composite Membranes. Polymeric Materials Science and Engineering **1995,** *11* (1), 7–14. (in Chinese).
17. Lu, W.J.; Liu, L.; Wang, H.; Ma, M.J. Study on Effect of the Structure Parameters of Asymmetric Polymer Membrane and Its Composite Membrane on Gas Separation. Polymeric Materials Science and Engineering **1994,** *10* (5), 96–102. (in Chinese).

Received November 2000
Revised March 2001

Request Permission or Order Reprints Instantly!